MALAYSIAN JOURNAL OF MICROSCOPY

Journal homepage: https://malaysianjournalofmicroscopy.org

RESEARCH ARTICLE

FUNGAL DERIVED CHITOSAN/ CELLULOSE NANOCRYSTALLINE BIOCOMPOSITES: ENHANCING WATER RESISTANCE AND MECHANICAL PROPERTIES

Kuan Eng Hoe[1], Sam Sung Ting[1,2,*], Noorulnajwa Diyana Yaacob[1], Madah Hussain[1], Wan Muhammad Aliif[1]

[1] Faculty of Chemical Engineering & Technology, Universiti Malaysia Perlis (UniMAP), 02600 Arau, Perlis, Malaysia.

[2] Centre of Excellence Geopolymer and Green Technology (CEGeoGTech), Universiti Malaysia Perlis, 02600 Arau, Perlis, Malaysia.

Abstract. Chitosan, a natural polymeric material, is widely used in packaging applications as it is good in barrier, optical, and mechanical properties. Traditionally, crustacean shells serve as the primary source for chitosan production using intensive acid and alkali treatments during its production. Furthermore, the commercial viability of chitosan production is hindered by fluctuations in both the quantity and quality of available crustacean shell waste, as well as the seasonal availability of this substrate, which can impact chitosan yield. In the current study, *Agaricus bisporus* fungal mushroom was used as a source for chitosan extraction. Fungal-derived chitosan (FCH) and cellulose nanocrystalline (CNC) biocomposite films were prepared and characterized using tensile test, Fourier Transform Infrared Spectroscopy (FTIR) and scanning electron microscopy (SEM). However, the tensile strength and the water resistance of fungal derived chitosan is relatively lower compared to crustacean based chitosan. Therefore, the incorporation of cellulose nanocrystalline (CNC) has successfully improved approximately 90% of the tensile strength using 4 wt% of CNC content. The water resistance of the composite has increased after the addition of CNC. Upon the findings, FTIR analysis confirms the presence of fungal chitosan's functional group. The FTIR spectra also showed the functional group of CNC in the composites. The micrograph of scanning electron microscopy (SEM) also indicated the good interfacial adhesion between composites film at 4 wt% NCC content. Therefore, the enhanced fungal derived chitosan (FCH) biocomposites could serve as suitable materials in food packaging.

Keywords: *Agaricus bisporus*, fungal derived chitosan, paddy straw.

Article Info

Received 15 January 2025
Accepted 28 February 2025
Published 2 June 2025

***Corresponding author: stsam@unimap.edu.my**

ISSN: 1823-7010, eISSN: 2600-7444

1. INTRODUCTION

Microplastic pollution, originating from discarded plastics, has become an escalating environmental concern. Although the specific toxicological mechanisms remain largely unclear, elevated concentrations of microplastics have been shown to adversely affect aquatic organisms and disrupt ecological balance [1], undermining the sustainability of environmental development. In response to this crisis, there is growing interest in developing biodegradable materials that align with green packaging principles. The packaging industry, accounting for a substantial share of global plastic production, often relies on short-lifespan materials, especially for products like fresh produce. Consequently, the development of bio-based and biodegradable packaging materials is essential to paving the way for a cleaner and more sustainable future.

Chitosan, derived from chitin, is the world's second most abundant natural polymer and it is renowned for its ability to form films. Chitosan exhibits a range of film-forming, functional, and biological properties [2]. Unlike marine-derived chitosan, fungal chitosan offers a vegan-friendly alternative, free from allergens such as tropomyosin, myosin light chain, and arginine kinase. Moreover, fungal chitosan provides enhanced control over its physicochemical properties, making it a versatile material for diverse applications. Mushrooms, as macro-fungi, are rich sources of chitin, which can be easily converted into chitosan. Among these, *Agaricus bisporus* (button mushroom) represents 40% of global edible mushroom production. Additionally, *Agaricus bisporus* is a significant reservoir of bioactive compounds, including phenols, sugars, vitamins, carotenoids, and minerals, which provide functional benefits and reduce the risk of various diseases, enhancing overall health. However, Chitosan has low water resistance, as well as poor mechanical and thermal properties, further restricting its use in functional film applications [3].

To overcome these limitations, cellulose nanocrystals (CNCs) are highly regarded for their exceptional properties, including a high length-to-width aspect ratio (10–100), a robustly interlinked network structure, superior optical transparency, and outstanding mechanical properties such as high tensile strength and stiffness, making them ideal as advanced reinforcement agents [4]. CNCs are sustainable nanomaterials distinguished by remarkable tensile strength, stiffness, and versatile surface functional groups, compatibility with chitosan, enabling a wide range of functional modifications. Their nanoscale dimensions confer unique advantages, making CNCs superior for applications such as high-performance nanocomposite reinforcement, polymeric emulsifiers in oil-water emulsions, and other advanced systems that surpass traditional materials [5]. CNCs form hydrogen bonds with chitosan, restricting polymer chain mobility, which enhances mechanical strength and improves water resistance by increasing the tortuosity of water vapor diffusion pathways [6].

The objective of this study is to produce FCH/CNC biocomposite films and evaluate their performance with varying CNC concentrations (0–10 wt%). The mechanical, chemical, and structural properties of the films were analyzed using tensile testing, Fourier-transform infrared spectroscopy (FTIR), and scanning electron microscopy (SEM). We hypothesized that incorporating CNC would enhance the tensile strength and reduce the water uptake of the FCH/CNC biocomposite films. The findings may contribute to advancing sustainable, bio-based materials for eco-friendly packaging applications.

2. MATERIALS AND METHODS

2.1 Materials

The cellulose source that was used in this study was paddy straw, it was collected from paddy fields nearby Perlis, Malaysia. The straw was ground and sieved to a particle size of 125 µm. The sieved particles were then soaked in water for 24 hours. The particles was oven dried at 80 °C. Mature fruiting bodies of *Agaricus bisporus* mushrooms were collected from the coastal area of Kuala Perlis, Malaysia. Hydrogen peroxide, glycerol, sulfuric acid were sourced from Merck (Darmstadt, Germany).

2.2 Fungal Chitosan Preparation

The fruiting bodies of *Agaricus bisporus* mushrooms were washed several times, blotted dry, lyophilized, and ground into a fine powder using a blender. The powder was stored at -20 °C until further use. The dried *Agaricus bisporus* powder was then homogenized in deionized water and sonicated. The resulting suspension was centrifuged, and the precipitate was subjected to deproteinization by treatment with sodium hydroxide at 100 °C for 2 hours. This deproteinization step was repeated to ensure complete removal of proteins from chitin. The mixture was subsequently washed with deionized water and centrifuged again. Decolorization was performed using a hydrogen peroxide solution. For N-deacetylation, the chitin was treated with a 30 wt% sodium hydroxide solution at 100 °C for 2 hours. After filtration, the chitosan was washed with deionized water until it reached a neutral pH, then freeze-dried [7]. Figure 1 presents a schematic diagram outlining the preparation process, which includes three main stages: extraction of chitosan from *Agaricus bisporus*, production of cellulose nanocrystals (CNC) from rice straw, and the subsequent formation of the FCH/CNC composites film.

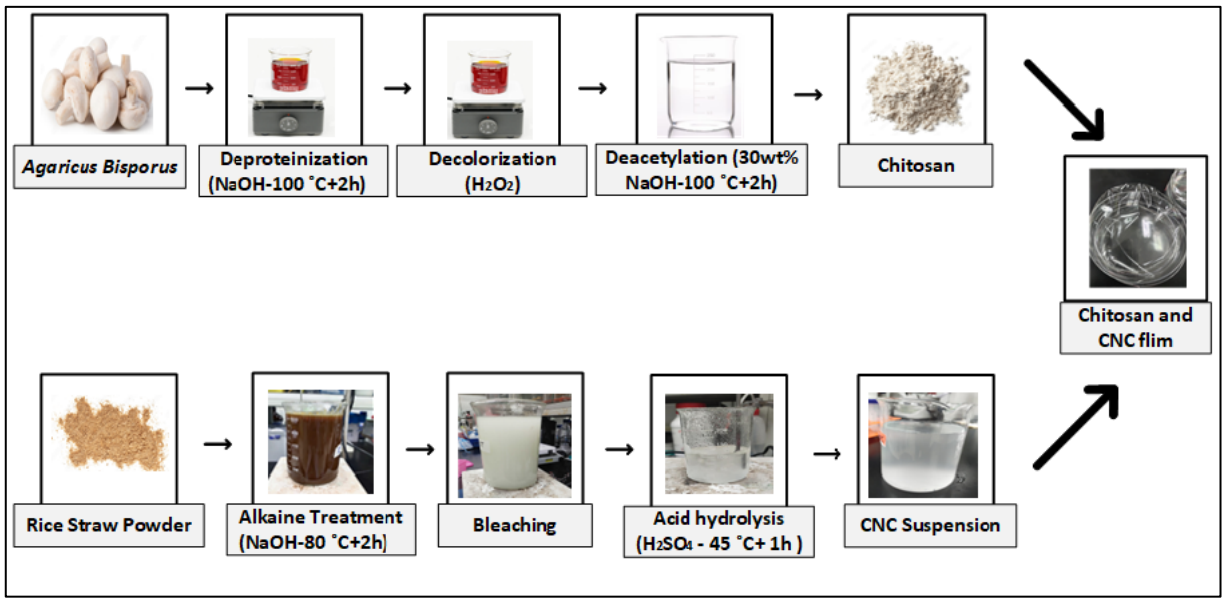

Figure 1: Preparation of FCH/CNC composite film

2.3 Isolation of Cellulose Nanocrystalline (CNC)

Two treatments were applied to rice straw which are alkaline treatment and bleaching treatment. Therefore, acid hydrolysis was used to separate the CNC from the rice straw fibre.

2.4 Alkaline Treatment

The purpose of alkaline treatment is to remove the lignin dan silica in the rice straw fibre. In this treatment, 40 g of rice straw fibre (powder) was treated with an alkaline treatment by dissolving 32 g of sodium hydroxide (NaOH) (4% w/v) in 800 ml of distilled water in a 1: 20 ratio. This treatment was stirred for 2 hours at 80 °C at a rate of 350 rpm. Following that, the fibre was filtered and washed with distilled water until it reached pH [8].

2.5 Bleaching Treatment

The alkaline-treated mixture was mixed and stirred in the prepared bleaching solution. An acetic buffer, 1.7% (w/v) NaClO2, and distilled water make up a bleaching solution. First, an acetic buffer was made with 40 g of sodium hydroxide, 75 mL of acetic acid, and 925 mL of distilled water.

The bleaching solution was prepared by combining the acetic buffer, $NaClO_2$, and distilled water in a 1:1:1 ratio, each with a volume of 267 ml. The alkaline treatment mixture was mixed with the bleaching solution and stir at 350 rpm for 2 hours at 80 °C. The treated fibre was thoroughly cleaned using distilled water. To obtain the white color form of fibre, the alkaline and bleaching treatments was cyclically repeated for two rounds. Then, the fibre was dried in the oven for 24 hours at 60 °C [9].

2.6 Acid Hydrolysis

The bleached fibre was subjected to acid hydrolysis in order to remove cellulose and remaining hemicelluloses and extract crystalline particles from a variety of cellulose sources. In this treatment, 2 g of cotton-like dried treated rice straw fibre was blended and add to sulfuric acid (64 wt%) at 45 °C for 1 hour at a consistent 700 rpm stirring rate. The solution was treated with 500 ml of cold distilled water to halt the reaction process. The suspension was obtained after the solution was kept at room temperature for at least 30 minutes. The hydrolysis process was halted by adding cold distilled water to the reaction mixture. The resulting suspension was centrifuged at 9000 rpm for 12 minutes in order to eliminate the excessive sulfuric acid. This centrifugation step was repeated multiple times until the supernatant became turbid. The pH of the supernatant reached 5 at the end of the centrifugation process. To prevent aggregation, the cellulose nanocrystal (CNC) suspension underwent ultrasonication for 10 minutes and was subsequently stored in a refrigerator at 4 °C [10].

2.7 CNC/ FCH Film Preparation

Fungal chitosan (FSH) was extracted from *Agaricus bisporus* with an approximate yield of 24.5% based on the dry weight. Approximately 2.25 g of FCH powder was mixed with 150 ml of distilled water to prepare a 1.5% (w/v) chitosan solution. The mixture was treated with 3 ml of 2% (v/v) acetic acid and stirred for 5 hours at 700 rpm at 60 °C. During the fourth hour of stirring, glycerol at a concentration of 10 wt% was incorporated into the solution to enhance the pliability of the chitosan film. The beaker was wrapped in aluminum foil throughout the 5-hour stirring process. In each preparation of FCH, varying amounts of CNC (0, 2, 4, 6, 8, and 10 wt%) were added to the FCH solution. CNC was introduced during the fourth hour of stirring, immediately after the addition of glycerol. After 5 hours, the mixture was subjected to sonicator for 10 minutes to remove the air trapped. For analysis, the mixture was poured into two Petri dishes for replication. The film was subsequently subjected to oven drying at 50 °C with a period of 48 hours without fan circulation. The film thickness ranged from 0.036 mm for pure chitosan film to 0.060 mm for the 10 wt% FCH/CNC composite film.

2.8 Tensile Test

The tensile test was conducted using an Instron Universal Testing Machine (Instron 3366) at room temperature, following the ASTM D882 standard. A crosshead speed of 10 mm/min was employed. The rectangular samples were cut into a dimension of 10 cm in length and 1 cm in width. The tensile strength, elongation at break, and Young's modulus were measured. Five samples were tested for each composition.

2.9 Fourier Transform Infrared Spectroscopy (FTIR) Analysis

The infrared spectra of FCH and its composites were obtained over a wavenumber range of 4000 cm^{-1} to 650 cm^{-1} using a Perkin Elmer Spectrum 10 spectrophotometer. The spectra were recorded with 16 scans at a resolution of 4 cm^{-1}, utilizing the attenuated total reflectance (ATR) technique.

2.10 Scanning Electron Microscopy (SEM) Analysis

The tensile fracture surfaces of CNC-reinforced FCH biocomposites were examined using a scanning electron microscope (FEl Quanta 200F). Observations were carried out at an accelerating voltage of 5 kV and a magnification of 500×.

2.11 Water Absorption Test

The water absorption of the biocomposite films was investigated at 50% relative humidity and 30°C. First, each of the films were cut into 3 equal parts and their initial dry weight were taken. Then, all of samples were submerged into distilled water overnight, and the subsequent reading was taken the next day where the samples were then weighed periodically. Water absorption (W) of the biocomposite film was computed as follows:

$$W = \frac{W_t - W_d}{W_d} \quad (1)$$

where W is the rate at which the biocomposite films absorbs water at a given time, W_t is the weight of the wet material at a given time, and W_d is the weight of the dry material (g).

3. RESULTS AND DISCUSSION

3.1 Tensile Properties

The tensile strength of FCH/CNC composites film with different CNC content is shown in Figure 2. Tensile strength of the films was steadily increasing up to 4% and thereafter decreased. There were numerous parameters, including the type of reinforcement fiber, fiber aspect ratio, fiber–matrix interfacial adhesion, and fiber orientation within the composites, influence the mechanical properties of the materials [11]. The increase in tensile strength in the presence of CNC was anticipated due to the high surface area of CNC. In addition, the increase in tensile strength may be due to the effective dispersion of the CNC filler within the chitosan polymer matrix, which strengthens the interfacial adhesion and filler-matrix interaction [12,13]. The stress was transferred to the filler as a result of the excellent dispersion between the matrix and filler, enhancing the crosslinking process, and in turn creating a more robust network between the crosslinker and matrix. Talebi et al. [14] similarly reported that incorporating CNC into chitosan films led to a 52% increase in tensile strength, highlighting CNC's significant reinforcing effect on mechanical properties.

As the CNC content higher than 4 wt%, the CNC particles might aggregated and serve as stress concentrators. When the aggregated regions form, stress concentrators, where stress is concentrated form as well, which frequently results in failure [15]. Therefore, these regions bear a disproportionate share of the load when an external force is applied, which causes the composite to defect and reduces its overall tensile strength

Figure 3 displays the effect of the CNC on the elongation at break of FCH/CNC biocomposites. The elongation at break offers information on the material's toughness and flexibility because a higher elongation at break means that the material may bend more before breaking, which is considered advantageous for a variety of plastic applications. The elongation at break of the FCH/CNC biocomposites raised up to 2 wt% CNC content and thereafter decreased. According to Ha et al. [16], the CNC aggregation by Van der Waal's forces and resulted the formation of voids or air bubbles during casting procerss. Kusmono et al. [17] reported similar findings, where the elongation at break increased at 2% and 4% CNC content, but decreased at higher concentrations due to reduced polymer chain mobility CNC aggregation.

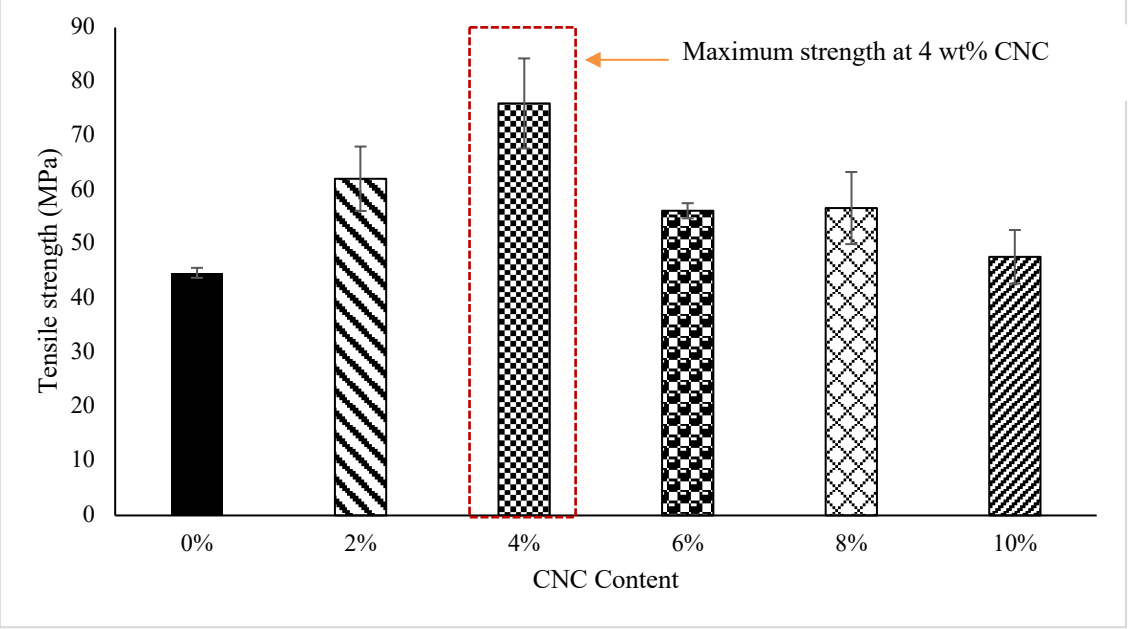

Figure 2: Tensile strength of FCH/CNC composites film with various CNC content

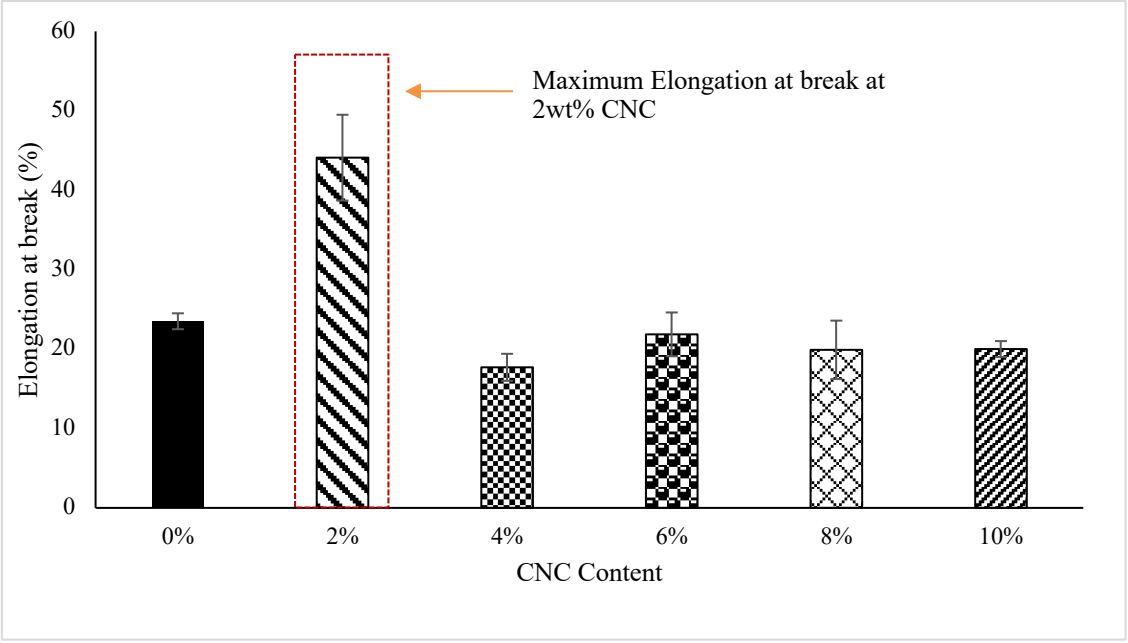

Figure 3: Elongation at break of FCH/CNC biocomposites with different CNC content

These factors affect the flexibility of the composites because stress transfer to the filler results in inefficient performance and may reduce its ductility. Gan et al. [18] revealed that the reduction in elongation at break was attributed to the stiffening effect of the CNC. Therefore, the mobility and flexibility of composites' polymer chains have been restricted by the inclusion of filler.

3.2 Morphological Analysis

Figure 4(a) to (d) presents the SEM micrographs of the tensile-fractured surfaces of FCH/CNC biocomposites with varying CNC content. Figure 4(a) shows a smooth surface for neat chitosan, while Figure 3(b) reveals a rougher fractured surface in the 4 wt% CNC biocomposite, indicating good surface interaction between FCH and CNC. With increasing CNC content, the surfaces appear progressively rougher and displayed the presence of pores (Figures 4(c)-(d)), which correlates with a reduction in elongation at break at higher CNC content. These findings align with the elongation at break data shown in Figure 3.

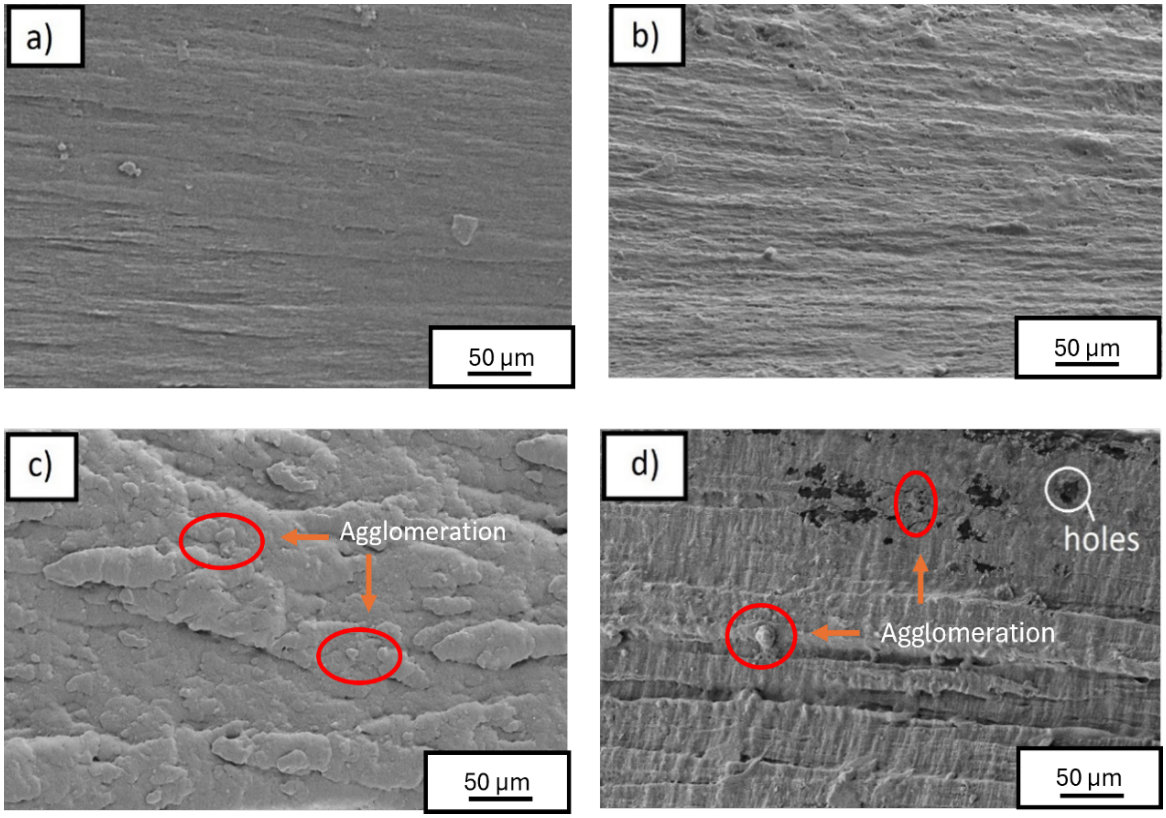

Figure 4: SEM micrographs of FCH/CNC biocomposites with (a) CNC 0 wt%, (b) CNC 2 wt%, (c) CNC 6 wt%, and (d) CNC 10 wt%

3.3 FTIR Analysis

Figure 5 shows the FTIR spectra of FCH/CNC biocomposites. In general, the peaks at 3200-3600 cm^{-1} were related to O-H stretching vibrations. The peaks are present at about the same range for all of the samples, indicating consistent hydroxyl group presence. As can be seen from pure CNC, the O-H peak is assigned at 3274.90 cm^{-1}, while it slightly decreases to 3261.09 cm^{-1} for 10 wt% CNC, and it continues to shift downwards to 3190.69 cm^{-1} for 2 wt% CNC. This shift suggests interaction bonding between CNC and chitosan matrix in the sample that plays a vital role for the availability of hydroxyl groups. Meanwhile between 2 wt% CNC and 10 wt% CNC, the peak's O-H intensity rose, suggesting that there might have been structural changes or the emergence of extra hydroxyl groups. These could have resulted from interactions between CNC and FCH that exposed or produced new hydroxyl groups [19].

In addition, peak that are shown in between 3200 cm^{-1} to 3100 cm^{-1} are usually an indicator for C-H stretching vibration and it appears in both cellulose and chitosan. From the spectra, the peak intensity of neat FCH (0 wt% CNC) are lower than the biocomposites with CNC. The peak presents in

between 1470 cm^{-1} to 1570 cm^{-1} represents amide II, in which it corresponds to the N-H group of secondary amines. In proteins and peptides, it is mainly linked to the N-H bending vibrations combined with the C-N stretching vibrations. Therefore, it acts as a functional peak of the presence of chitosan [20]. However, the similar peak can also be observed in neat CNC sample, at 1542.20 cm^{-1}. The absorption peak or band between 1000 cm^{-1} to 1150 cm^{-1} represented the C-O group. The β-1,4-glycosidic bond in the cellulose polymer chain is thought to be the source of the C-O-C stretching vibrations that give rise to the peak of 1028.95 cm^{-1} for pure CNC, which is frequently observed in cellulose materials. The subsequent drop in intensity peak between the biocomposites with 2 wt% CNC and 10 wt% CNC can be a sign of exposure to previously shielded C-O groups. Additional interactions or reactions between the system's components contributed to the intensity reduction [21].

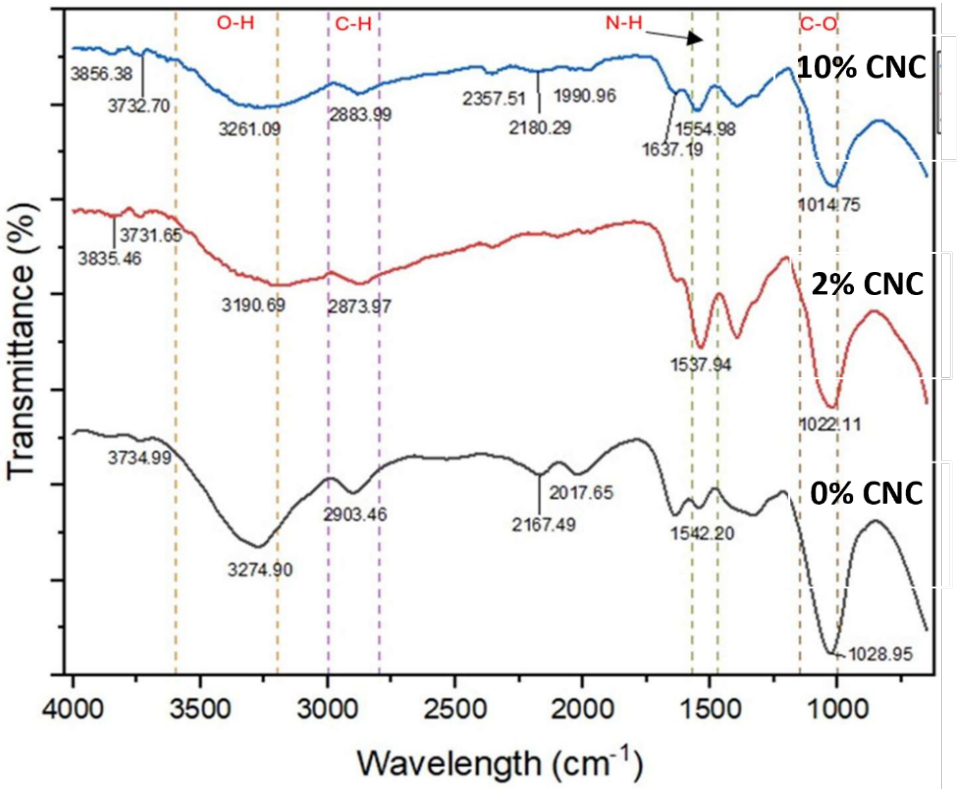

Figure 5: FTIR spectra of (a) neat FCH, (b) 2wt% CNC and (c) 10wt% CNC biocomposites

3.4 Water Absorption

Water absorption is the measurement of the water-absorbing capacity of the biocomposites, demonstrating the films' capacity to take in water from the surrounding environment. Figure 6 depicts the water update of FCH/CNC biocomposites with different CNC content. The figure indicated that neat chitosan (0 wt% CNC) exhibited the highest initial water uptake, recorded nearly at 900% on day 1. From there onwards, there was a noticeable decline in water uptake over 9 days, before it stabilized around 300% at the end of the water absorption test period. The reduction can be related to the significant water loss or desorption over time due to evaporation of water. On the other hand, biocomposites with 2 wt% CNC and 4 wt% CNC acts almost the same as both content uptake spikes up to 500% on day 1 and remains relatively stable for the whole 9 days, fluctuating but staying in the range of 450 – 500%. This stability indicates that these percentage are ideal for consistent water absorption and retention behavior. Overall, the increase of CNC content had subsequently reduced the water uptake of FCH/CNC biocomposites.

According to Chi et al. [22], the enhanced interfacial bonding between CNC and chitosan introduced a more convoluted pathway in the composite films, significantly impeding water vapor

diffusion. As illustrated in Figure 5, the addition of CNC formed a complex interconnected matrix, further increasing the tortuous diffusion pathway for water vapor through the chitosan composite film. As a result, the water absorption of the FCH/CNC films was significantly reduced. Mao et al. [6], who reported that the incorporation of 5 wt% CNC into chitosan membranes resulted in approximately a 50% reduction in swelling, attributed to increased crystallinity and strong interfacial interactions that hinder water permeation.

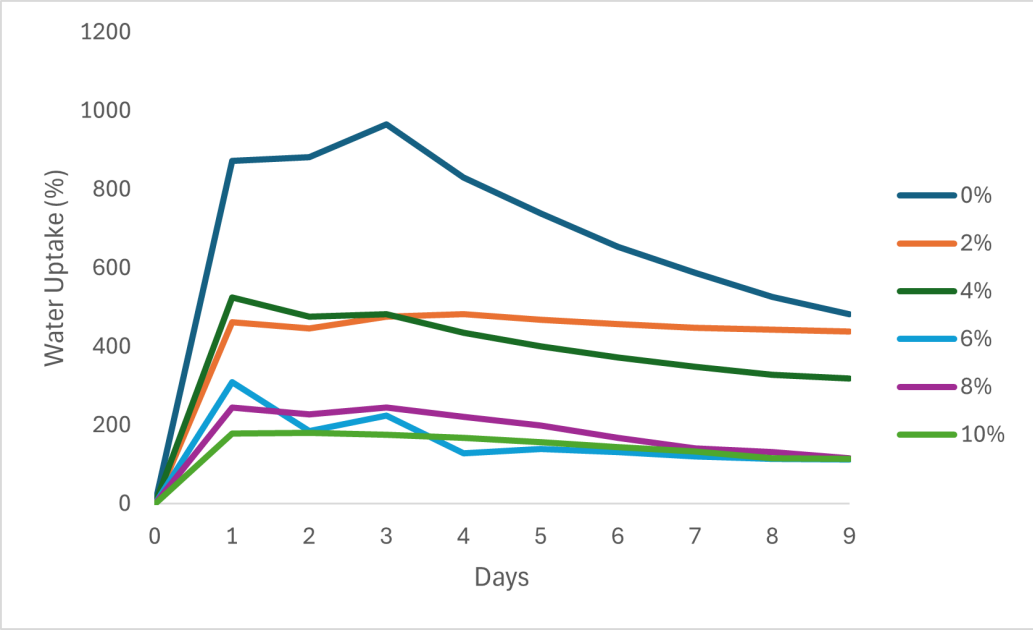

Figure 6: Water uptake of FCH/CNC biocomposites varying with CNC content

4. CONCLUSIONS

In conclusion, the FCH/CNC biocomposite films demonstrated the optimal tensile strength at a CNC content of 4 wt%, achieving a ~90% increase in tensile strength and improved water resistance. Whereas the composites with 2 wt% CNC showed the highest elongation at break. SEM micrographs strong interfacial adhesion at 4 wt% CNC, supporting the structural integrity of the films. Furthermore, biocomposites with higher CNC content displayed pores on the fractured surface. Additionally, the water absorption of the FCH/CNC composites film was lessened with the addition of CNC, enhancing the water resistance of the composites. These findings suggest that FCH/CNC biocomposite films possess enhanced mechanical and water-resistant properties, making them promising candidates for applications in biodegradable packaging materials and other environmentally friendly solutions. These FCH/CNC biocomposites are renewable, biodegradable, and non-toxic, making them superior to conventional petroleum-based plastics. However, CNC agglomeration at higher loadings may reduce composite performance.

Acknowledgements

The authors wish to thank to the research funding namely Fundamental Research Grant Scheme (FRGS/1/2022/TK09/UNIMAP/02/21) from Ministry of Higher Education Malaysia.

Author Contributions

All authors contributed toward data analysis, drafting and critically revising the paper and agree to be accountable for all aspects of the work.

Disclosure of Conflict of Interest

The authors declare no potential conflict of interest in the publication of this work.

Compliance with Ethical Standards

The work is compliant with ethical standards.

References

[1] Sen Gupta, R., Samantaray, P. K. & Bose, S. (2023). Going beyond cellulose and chitosan: synthetic biodegradable membranes for drinking water, wastewater, and oil–water remediation. *ACS Omega*, 8(28), 24695-24717.

[2] Lin, D., Zheng, Y., Huang, Y., Ni, L., Zhao, J., Huang, C., Chen, X., Chen, X., Wu, Z., Wu, D., Chen, H., Zhang, Q., Qin, W. & Xing, B. (2020). Investigation of the structural, physical properties, antioxidant, and antimicrobial activity of chitosan–nano-silicon aerogel composite edible films incorporated with okara powder. *Carbohydrate Polymers*, 250, 116842.

[3] Grimm, D. & Wösten, H. A. (2018). Mushroom cultivation in the circular economy. *Applied Microbiology and Biotechnology*, 102, 7795-7803.

[4] Sharma, G., George Joy, J., Sharma, A. R. & Kim, J. C. (2024). Accelerated full-thickness skin wound tissue regeneration by self-crosslinked chitosan hydrogel films reinforced by oxidized CNC-AgNPs stabilized pickering emulsion for quercetin delivery. *Journal of Nanobiotechnology*, 22(1), 323.

[5] Baek, J., Wahid-Pedro, F., Kim, K., Kim, K. & Tam, K. C. (2019). Phosphorylated-CNC/modified-chitosan nanocomplexes for the stabilization of Pickering emulsions. *Carbohydrate Polymers*, 206, 520-527.

[6] Mao, H., Wei, C., Gong, Y., Wang, S. & Ding, W. (2019). Mechanical and water-resistant properties of eco-friendly chitosan membrane reinforced with cellulose nanocrystals. *Polymers*, 11(1), 166.

[7] Affandy, M. A. M. & Rovina, K. (2024). Characterization of chitosan derived from mushroom sources: Physicochemical, morphological, thermal analysis. *Sustainable Chemistry and Pharmacy,* 40, 101624.

[8] Khaleghian, H., Molaverdi, M. & Karimi, K. (2017). Silica removal from rice straw to improve its hydrolysis and ethanol production. *Industrial & Engineering Chemistry Research*, 56(35), 9793-9798.

[9] Romruen, O., Karbowiak, T., Tongdeesoontorn, W., Shiekh, K. A. & Rawdkuen, S. (2022). Extraction and characterization of cellulose from agricultural by-products of Chiang Rai Province, Thailand. *Polymers*, 14(9), 1830.

[10] Zulkifli A.S., Abd Halim N.A., Ibrahim S., Hamzah N. & Saleh S.H. (2024). Effect of sulphuric acid concentration on nanocellulose extraction from rice husk. *Malaysian Journal of Chemistry*, 26(5), 562 - 571

[11] Chie, S. & Ab Wahab, M. K. (2019). Morphology and biodegradability of microcrystalline cellulose/chitosan films. IOP Conference Series: *Materials Science and Engineering*, 701(1), 012053.

[12] Li J., Shen C. & Li X. (2021). Preparation and optimization of modified chitosan composite film. *Science and Technology of Food Industry*, 42(8), 144 – 151.

[13] Luo, Y., Wang, J., Lv, T., Wang, H., Zhou, H., Ma, L. & Dai, H. (2023). Chitosan particles modulate the properties of cellulose nanocrystals through interparticle interactions: Effect of concentration. *International Journal of Biological Macromolecules*, 240, 124500.

[14] Talebi H, Ghasemi F. A. & Ashori A. (2021). The effect of nanocellulose on mechanical and physical properties of chitosan-based biocomposites. *Journal of Elastomers & Plastics*, 54(1), 22-41.

[15] Ghayoor, H., Hoa, S. V. & Marsden, C. C. (2018). A micromechanical study of stress concentrations in composites. *Composites Part B: Engineering*, 132, 115-124.

[16] Ha, N. T. T., Giang, N. T. K., Ha, N. N. & Lan, P. T. (2023). Understanding the interaction in cellulose–chitosan composite and its adsorption ability for nickel(II): a theoretical investigation. *Molecular Simulation*, 49(13-14), 1303-1310.

[17] Kusmono, Wildan M. W. & Lubis F. I. (2021). Fabrication and characterization of chitosan/cellulose nanocrystal/glycerol bio-composite films. *Polymers*, 13(7), 1096.

[18] Gan, P. G., Sam, S. T., Abdullah, M. F., Omar, M. F., & Tan, W. K. (2020). Comparative study on the properties of cross-linked cellulose nanocrystals/chitosan film composites with conventional heating and microwave curing. *Journal of Applied Polymer Science*, 137(48), 49578.

[19] Beji, E., Keshk, S., Douiri, S., Charradi, K., Ben Hassen, R., Gtari, M., Attia, H. & Ghorbel, D. (2023). Bioactive film based on chitosan incorporated with cellulose and aluminum chloride for food packaging application: Fabrication and characterization. *Food Bioscience*, 53, 102678

[20] Ji, Y., Yang, X., Ji, Z., Zhu, L., Ma, N., Chen, D., Jia, X., Tang, J. & Cao, Y. (2020). DFT-calculated IR spectrum amide I, II, and III band contributions of N-methylacetamide fine components. *ACS Omega*, 5(15), 8572-8578.

[21] Huang, X., Xie, F. & Xiong, X. (2018). Surface-modified microcrystalline cellulose for reinforcement of chitosan film. *Carbohydrate Polymers*, 201, 367-373.

[22] Chi, K. & Catchmark, J. M. (2018). Improved eco-friendly barrier materials based on crystalline nanocellulose/chitosan/carboxymethyl cellulose polyelectrolyte complexes. *Food Hydrocolloids*, 80, 195-205.